

Combination of a Full-Wave Method and Ray Tracing for Radiation Pattern Simulations of Antennas on Vehicle Roofs

Marina S. L. Mocker (marina.mocker@tum.de)¹, Manuel Schiller², Robert Brem¹, Zuguang Sun¹, Hicham Tazi³, Thomas F. Eibert¹, Alois Knoll²

¹Lehrstuhl für Hochfrequenztechnik, Technische Universität München

²Lehrstuhl für Echtzeitsysteme und Robotik, Technische Universität München

³AUDI AG, Ingolstadt

Abstract—An electromagnetic simulation approach combining a full-wave method with ray tracing is presented. This is used to simulate the radiation characteristic of a roof antenna system on a vehicle roof. The radiated fields of the antenna are first simulated for example with CST Microwave Studio (MWS) or measured and then utilized in the ray tracer. Besides to the modeling of the roof itself, also the antenna patterns are investigated. Small distances between the antenna and the vehicle roof do not allow to work with far-field assumptions. In this case, antennas with reduced extents are used, called subtransmitters [1]. These subtransmitters are represented by surface currents obtained from simulations with CST MWS. With this concept, also an antenna on the roof can be simulated with a ray tracing approach. Finally, more accurate results can be gained in Virtual Test Drive simulations. Furthermore, the simulation of radiation characteristics of vehicle roof antennas can be accelerated.

I. INTRODUCTION

Future car generations will be equipped with wireless communications links to exchange information among cars and between cars and infrastructure to improve road safety and travel efficiency. These communication systems will require highly complex antenna systems which support diversity and multiple input multiple output (MIMO) systems. The performance of these future communication systems will strongly depend on reliable physical channel simulations. The capability to perform the simulation of communication channels in Virtual Test Drive simulations is essential for automotive engineering in the field of communications in order to cope with reduced development cycles and increasingly complex systems. By means of these simulations, antenna systems related questions like antenna positioning [2] can be optimized and important information such as coverage can be gained. Approximating the interaction of a plane wave with an antenna allows the assessment of the suitability of antenna positions [3]. However, for an even more accurate optimization of antenna systems by simulations, a more precise modeling of the radiation from the vehicle antenna, which takes into account coupling effects, is necessary. In case the antenna is coupled with its environment, a reliable simulation of the radiation characteristics requires high computational effort and, as a consequence, long simulation times when employing full-wave electromagnetic

simulation methods.

A good approximation for the propagation of electromagnetic waves is offered by ray tracing [4]. The chosen ray tracing method is based on geometrical optics (GO) and the uniform geometrical theory of diffraction (UTD), where the rays represent the propagation of wave fronts. In areas close to complex discontinuities ray-based solutions are not sufficiently accurate and thus full wave methods can be used [5]. In this paper only the antenna is simulated with a full-wave method. The environment is taken into account by ray tracing which can highly accelerate the simulations. In order to introduce vehicle antennas both efficiently and accurately into ray tracing simulations, several investigations are presented in the following.

II. DESCRIPTION OF THE SIMULATION

The considered three-dimensional ray tracer is based on the shooting and bouncing rays method [6]. This is a brute force method, which is based on the tracing of a large number of rays, which are sent in random directions from the center point of each transmitting antenna to sample the three-dimensional space. As a ray propagates through the 3D scene, it can be reflected or refracted at surfaces, which are modeled through triangle meshes with additional material information. Additionally, diffraction at metallic [7] or dielectric edges [8] can occur. Receiving antennas are modeled as spheres, so a ray hitting such a sphere is considered as received. The accuracy of this method increases with the number of rays sent. As the calculations which are necessary for ray tracing are highly-parallelizable [4], graphic processing unit (GPU) computing is employed to allow a large number of rays to be processed in parallel, which results in a significant reduction of simulation time. As a preprocessing step, a dipole antenna at 2.4 GHz and 5.9 GHz is simulated with CST MWS [9] and the resulting antenna pattern is exported. In general, the pattern could also be simulated with other methods or it could be obtained from measurements. The antenna pattern is then imported into the ray tracer, along with the scene information describing position and orientation of transmitter and receivers, surface models

and material properties as well as geometrical information of the diffraction edges. In the investigated scenarios the receivers build a ring of isotropic receivers in 1° steps as shown in Fig.1. All diffracted rays are magenta, all reflected or refracted

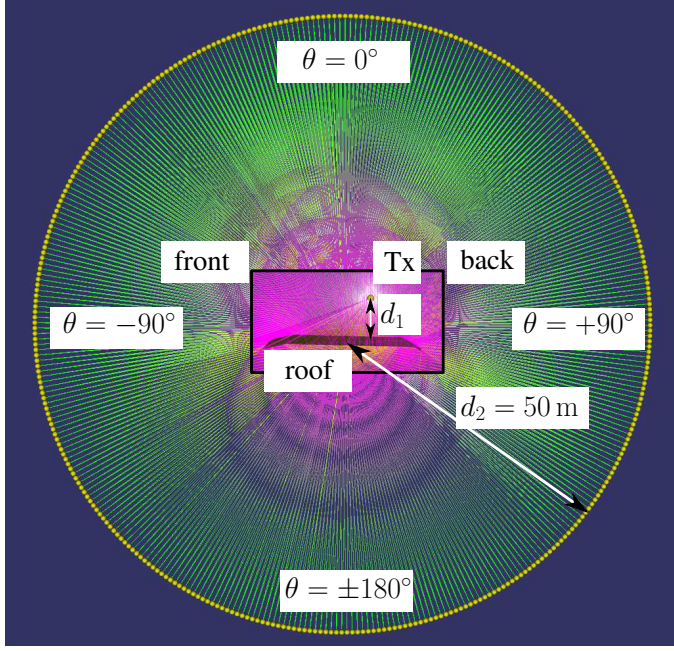


Fig. 1. Ring of receivers vertically around the roof ($\theta = -90^\circ$ is in front, $\theta = 90^\circ$ is backwards) with a simplified vehicle roof model and a transmitter

rays are yellow. A ray hitting a receiver turns green at the end. The electric fields received by the receiver ring in 50 m distance are compared with the electric fields simulated in CST MWS at the same distance. The minimum distance to fulfill the far field condition from Eq. (1) for a transmitting system consisting of the roof and the antenna at 2.4 GHz is ≈ 21 m, which is fulfilled for a receiver ring with a radius of 50 m. The investigation focuses on the simulation of the radiation pattern of an antenna mounted on a vehicle roof. For the simulations with CST MWS a work station with an Intel Core i7 and 12 GB random access memory (RAM) is used. For the GPU ray tracing simulations a NVIDIA GeForce GTS 750 Ti with 2 GB memory is used.

III. MODELLING OF CAR ROOFS FOR THE SIMULATION

For the purpose of simulations, car models are converted into NASTRAN format, where the geometry is composed of triangles shown in Fig. 2 in red. As the roof is slightly bent, each planar triangle would lead to diffraction edges, but the calculation of a huge number of diffractions leads to a high consumption of memory. Still rays hitting the outer edges of the roof and causing diffraction are necessary as the diffraction is dominant for propagation in non line of sight regions. In order to hit the outer edges, after diffractions one of the rays is propagated along the surface. Rays, which are propagating along the surface, cannot be separated in reflected and direct rays. Thus, the diffraction coefficients for the ray propagating

along the surface are modified [10]. It is not possible to efficiently carry out a simulation, where diffraction edges are defined for each triangle. Thus, simplifications are necessary, which are shown in Fig. 2. The first one is to define only diffraction edges at the outer boundary of the roof, which is shown by dashed green lines. The simulation configuration is shown in Tab. I, the material of the roof is perfect electrical conductor (PEC) and the antenna pattern is obtained by the radiation pattern of a vertically oriented dipole. A comparison

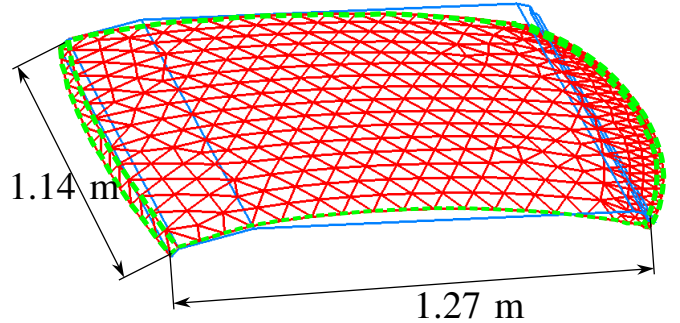


Fig. 2. Two car roof models with diffraction edges composed of triangles (red) and a simplified version (blue)

of the ray tracing results with the simulation results using the transient (T) solver in CST MWS at 50 m distance is shown in Fig. 3. Between -180° and -110° the number of rays hitting the outer boundary edge is not sufficient to achieve the same electric field level as in the CST MWS simulation. The overall bending of the roof is strong, thus, only a few rays hit the outer edge, which lead to diffraction in this angular range. The ray tracing simulation between -110° and -40° shows strong peaks resulting from reflections at single triangles. As the model is composed of flat triangles, the influence of the bending cannot be taken into account. In order to evaluate the

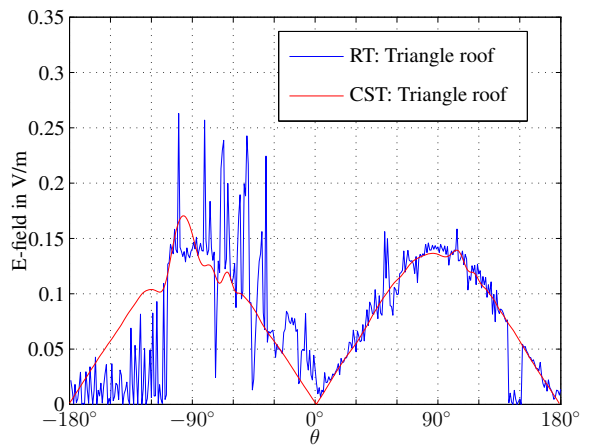


Fig. 3. Ray tracing and CST MWS simulation in a distance of $d_2 = 50$ m of the triangle roof at 2.4 GHz

ray tracing effects itself, a further simplification of the roof, shown in Fig. 2 in blue color, is investigated. Every line shown

TABLE I
SIMULATION OF THE ROOF CONSISTING OF TRIANGLES AND THE SIMPLIFIED ROOF

Simulation	Rays Sent	Diffracted Rays	Time	Memory
Triangles RT	20 000	2550	5 s	1.8 GB
Triangles CST	-	-	≈ 12 h	4.8 GB
Simplified RT	20 000	1 020	5 s	1.9 GB
Simplified CST	-	-	≈ 2 min	0.2 GB

is defined as a diffraction edge. The simulation configuration is shown in Tab. I with the same antenna configurations as in the simulation with the more detailed roof model. The results of CST MWS and modified ray tracing simulation show a high degree of agreement (see comparison in Fig. 4).

The time consumption, shown in Tab. I, does not change for both roofs in the ray tracer, but the amount of used GPU memory increases slightly as more diffractions are calculated. The ray tracing simulation is much faster than the simulation in CST MWS, but especially for complex models, the accuracy can decrease strongly.

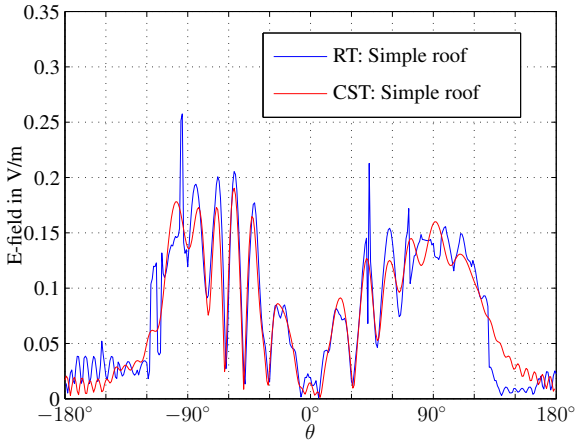


Fig. 4. Ray tracing and CST MWS simulation in a distance of $d_2 = 50$ m of the simplified metal roof at 2.4 GHz

IV. INFLUENCE OF FAR FIELD CONDITIONS

The ray tracing simulation for the propagation of electromagnetic waves assumes locally plane waves. This is fulfilled for large distances from the last intersection, but not in the near field region. This has a strong influence on the accuracy of ray tracing simulations. To assume field propagation as locally plane waves the phase difference between all wave contributions must be less than $\lambda/16$ [11] which is a typical definition for the plane wave assumption. As the excitation over the whole surface contributes to the radiation, the phase difference between the waves radiated at the most distant points of the aperture L is relevant. With a maximum phase difference of $\lambda/16$ it is possible to calculate the minimum distance

$$d_{ff} \geq \frac{2L^2}{\lambda} \quad (1)$$

to fulfill this condition. Furthermore, for a correct calculation of the intersection coefficients, like for example diffraction or reflection, it is necessary, that the wavelength is small compared to the dimensions of the structure. The assumption for the diffraction coefficients calculated with UTD is an infinite edge. Also for the reflection coefficients, the plane must be large compared to the wavelength. The simulation, where the influence of this assumption is investigated, is shown in Fig. 5. The roof consists of metal parts framing a

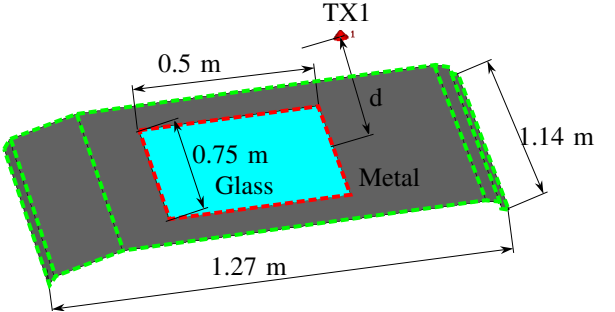


Fig. 5. Car roof with a panorama window and diffraction edges for metal (green) and glass (red)

glass window. The metal diffraction edges in green color are calculated with UTD [7] and the diffraction edges surrounding the glass, shown in Fig. 5 in red color, are calculated with heuristic diffraction coefficients [8] taking into account dielectric properties. Both materials do not have a roughness, the relative permittivity of metal is defined as $\epsilon_r = 1 - j10^{10}$. For glass a relative permittivity of $\epsilon_r = 4.82 - j0.026$ [9] is used. Again, a dipole is used and the distance d_1 between the dipole and the roof is 0.329 m, which fulfills the far field condition in Eq. (1) at 2.4 GHz resulting in $d_{ff} \geq 0.625$ m. Also the far field condition for the distance d_2 between the complete roof and the receiver ring is fulfilled. The minimum distance $d_{ff} \geq 21$ m and the used distance is 50 m. The scenario is simulated at 2.4 GHz and 5.9 GHz, where the far field conditions are fulfilled even better. In Fig. 6 the car roof with the panorama window, all diffractions edges and all rays are shown. The simulation with ray tracing is

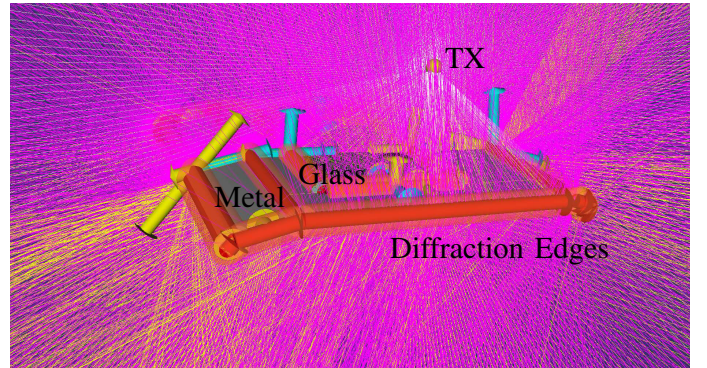


Fig. 6. Car roof with a panorama window, diffraction edges and all received rays

increasingly advantageous regarding the time consumption at

TABLE II
SIMULATION OF A ROOF WITH A PANORAMA GLASS WINDOW

Simulation	Frequency	Rays Sent	Diffracted Rays	Time	Memory
RT	2.4 GHz	20 000	1 020	5 s	1.8 GB
CST	2.4 GHz	-	-	613 s	4.2 GB
RT	5.9 GHz	20 000	1 020	5 s	1.8 GB
CST	5.9 GHz	-	-	5323 s	4.3 GB

higher frequencies. The CST simulation at 5.9 GHz takes much longer than the simulation with ray tracing as shown in Tab. II. The necessary computation time for the ray tracing simulation is independent of the simulated frequency. The influence of the far field conditions and the ratio between wavelength and the dimensions of the vehicle are investigated with the two identical simulations, apart from the dipole frequency, shown in Fig. 7 for 2.4 GHz and Fig. 8 at 5.9 GHz. The simulation at

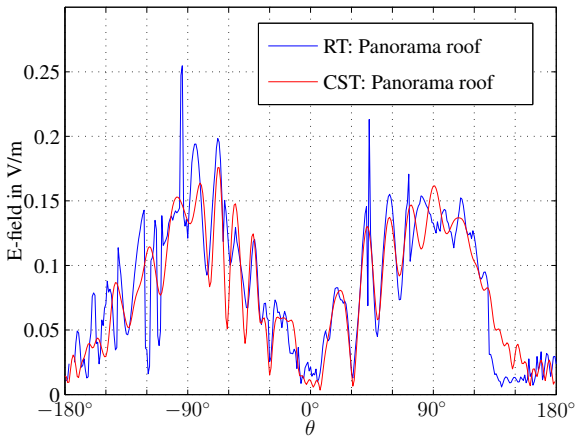


Fig. 7. Ray tracing and CST MWS simulation in a distance of $d_2 = 50$ m of the simplified panorama roof at 2.4 GHz

higher frequencies is more accurate concerning the amplitudes and the angle positions of the maxima and minima. These

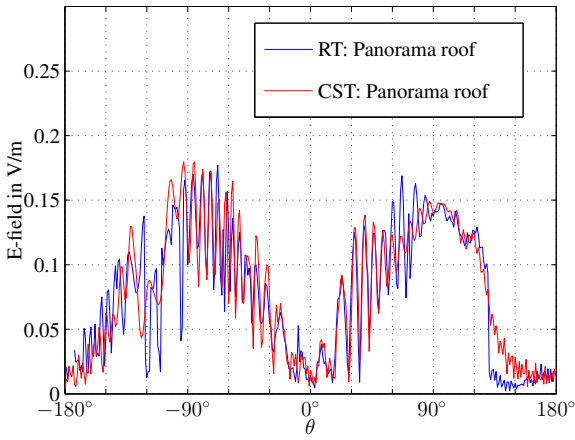


Fig. 8. Ray tracing and CST MWS simulation in a distance of $d_2 = 50$ m of the simplified panorama roof at 5.9 GHz

simulation evaluations show, that an accurate simulation of

vehicle roofs is possible. In all simulations up to now the antenna was located with a certain distance from the roof. This is usually not fulfilled for vehicle antennas, which are mounted directly on the car. Thus in the next step, the antenna is moved towards the roof to a distance $d_1 = 0.041$ m, which is much closer than the calculated far field distance 0.626 m calculated from Eq. (1). In this simulation, the simplified metal roof from Fig. 2 is used. The result is compared to the CST MWS simulation in Fig. 10 and as expected, the results show the same trend, but a higher accuracy could be achieved in the simulation, where the far field condition was fulfilled. The same effect can be observed in case the distance d_2 between the roof and the receiver ring is reduced, but the distance d_1 is more important for the overall accuracy. As the far field condition is dependent on the aperture L , this parameter can be changed by the introduction of subtransmitters, which subdivide the aperture into smaller areas, as shown in Fig. 9 [1]. By dividing the dipole into 9 subtransmitters, the far field

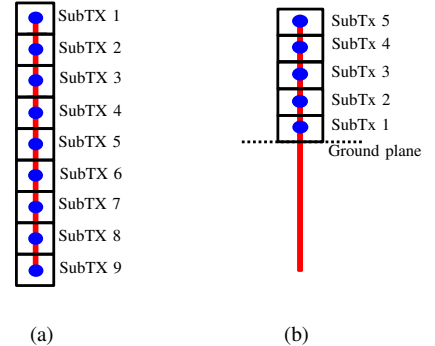


Fig. 9. Subtransmitters (blue) calculated from the surface currents on a dipole (red), the boxes which determine the allocation of the currents to one of the subtransmitters for the dipole simulation (a) and the monopole simulation (b)

distance d_{ff} is reduced drastically and is fulfilled as well for the lowest of the 9 subtransmitters. First, the antenna is simulated in CST MWS [9]. By means of the exported surface currents J_S , the patterns of the smaller transmitters can be calculated [1]. By use of the magnetic vector potential [12] the radiation patterns of the subtransmitters, represented by the electric field in 1 m distance are calculated [1]. The field values received by the receiver ring, shown in Fig. 1, are equal for all 9 subtransmitters and the dipole. As shown in Fig. 10, the simulation agrees very well with the simulation in CST MWS. The phase of all wave contributions can be calculated more accurately, which mainly has an influence on the distribution of the maxima and minima.

V. SIMULATION OF MONOPOLES WITH SUBTRANSMITTERS

In case the antenna is mounted on the roof and behaving similar to a monopole, no distance between the antenna and the roof is offered. The antenna port is positioned inside the roof, but the origin of a ray tracing simulation cannot be located within the structure. Thus, an approach must be found

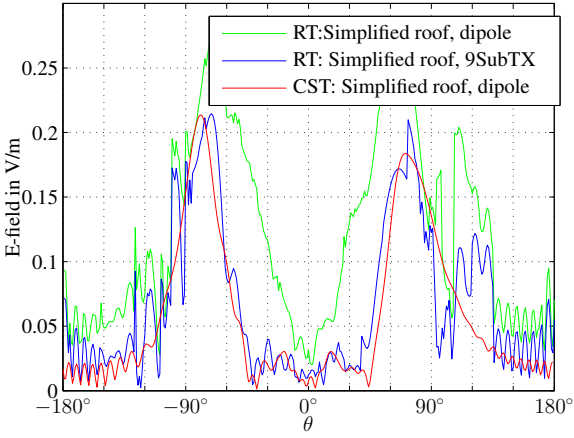


Fig. 10. Ray tracing and CST MWS simulation in a distance of $d_2 = 50$ m of the simplified panorama roof at 2.4 GHz with a dipole represented by a single antenna and with a dipole represented by 9 subtransmitters

to replace the position inside the structure by other positions. A monopole on an infinite plane behaves like a dipole in the upper hemisphere. The conducting plane is like a mirror and replaces the lower part of the dipole. Thus a dipole is simulated in CST MWS and the surface currents are exported. For the ray tracing simulation only boxes over the upper part of the dipole are used and 5 subtransmitters are defined as shown in Fig. 9(b). In the following the simulation of a monopole in the rear part of the roof of the simplified metal roof, as shown in Fig. 2 in blue color, is investigated. The 5 subtransmitters are located exactly in the same position as the monopole in the CST MWS simulation. The electric field values are shown in Fig. 11. For the calculation of the subtransmitters an infinite

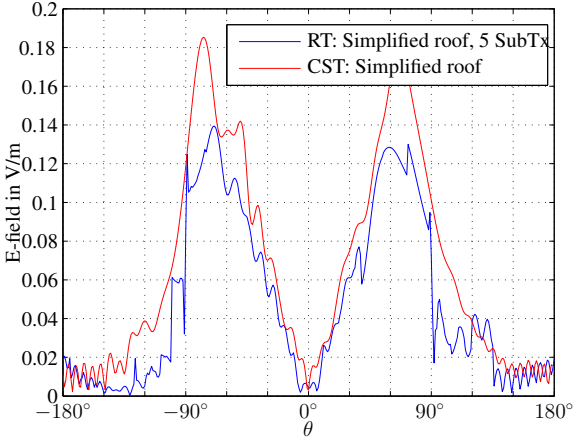


Fig. 11. Ray tracing and CST MWS simulation in a distance of $d_2 = 50$ m of the simplified panorama roof with a monopole at 2.4 GHz represented by 5 subtransmitters

plane was assumed, but in the final simulation the metal roof is used. As this roof also has influences on the coupling, the results do not match everywhere. Still, the simulation approach is useful to investigate strongly coupled antennas with ray tracing.

VI. CONCLUSION

An efficient way to simulate the radiation pattern of the antenna on a vehicle was presented. All ray tracing simulation results were compared to the full-wave transient solver of CST MWS in terms of efficiency and accuracy. The ray tracing based simulation allows the calculation of radiation patterns with very low time consumption. Concerning the accuracy, good results could be achieved for vehicle structures consisting of metal and constructed of planar pieces including diffraction edges. The assumption of transverse electromagnetic waves, which is basis of ray tracing, is no longer fulfilled if antennas are positioned close to the roof. This disadvantage of the simulation approach was solved by the use of subtransmitters and very good results with this modification could be shown. Also a monopole antenna, which is strongly coupled with the vehicle structure, was replaced by subtransmitters and a good simulation result could be presented. Consequently, accurate simulations with ray tracing, which also take into account near field effects, are possible with this approach. With this modeling also ray tracing simulations with high accuracy in a larger environment are possible. This is necessary for Virtual Test Drive simulations in order to optimize antenna systems or to investigate the physical channel in real-time.

REFERENCES

- [1] R. Brem and T. F. Eibert, "Multi-radiation center transmitter models for ray tracing," *IEEE Transactions on Antennas and Propagation*, vol. 60, no. 7, July 2012.
- [2] L. Reichardt, T. Fuegen, and T. Zwick, "Influence of antennas placement on car to car communications channel," in *3rd European Conference on Antennas and Propagation (EUCAP)*, March 2009.
- [3] L. Reichardt, J. Pontes, C. Sturm, and T. Zwick, "Simulation and evaluation of car-to-car communication channels in urban intersection scenarios," in *IEEE Vehicular Technology Conference*, May 2010.
- [4] T. J. Purcell, I. Buck, W. R. Mark, and P. Hanrahan, "Ray tracing on programmable graphics hardware," *ACM Trans. Graph.*, vol. 21, no. 3, pp. 703–712, Jul. 2002. [Online]. Available: <http://doi.acm.org.eaccess.ub.tum.de/10.1145/566654.566640>
- [5] Y. Wang, S. Safavi-Naeini, and S. K. Chaudhuri, "A hybrid technique based on combining ray tracing and ftd methods for site-specific modeling of indoor radio wave propagation," *IEEE TRANSACTIONS ON ANTENNAS AND PROPAGATION*, vol. 48, no. 5, pp. 743–754, May 2000.
- [6] K. R. Schaubach, N. J. Davis, and T. S. Rappaport, "A ray tracing method for predicting path loss and delay spread in microcellular environments," in *IEEE Vehicular Technology Conference*, May 1992.
- [7] R. G. Kouyoumjian and P. H. Pathak, "A uniform geometrical theory of diffraction for an edge in a perfectly conducting surface," *Proceedings of the IEEE*, vol. 62, no. 11, November 1974.
- [8] S. Soni and A. Bhattacharya, "New heuristic diffraction coefficient for modeling of wireless channel," *Progress in Electromagnetic Research*, vol. 12, pp. 125–137, April 2010.
- [9] CST AG, *CST MWS description*, <https://www.cst.com/Products/CSTMWS>.
- [10] Y. T. Lo and S. W. Lee, Eds., *Antenna Handbook, Theory, Applications, and Design*. Van Nostrand Reinhold Company Inc., 1988.
- [11] J. D. Kraus and R. J. Marhefka, *Antennas for all Applications*. McGraw-Hill, 2002.
- [12] C. A. Balanis, *Advanced Engineering Electromagnetics*, 2nd ed. John Wiley and Sons, 2012.